Journal of Polymer Research (2020) 27: 251
https://doi.org/10.1007/s10965-020-02231-0

ORIGINAL PAPER

Synthesis and characterization of pH responsive alginate based-hydrogels as oral drug delivery carrier

Pinar Ilgin[1] · Hava Ozay[2] · Ozgur Ozay[2,3]

Received: 18 December 2019 / Accepted: 26 May 2020 / Published online: 6 August 2020

Abstract

As pharmaceutical carrier materials having antibacterial and pH-sensitive properties, hydrogels have great potential for clinical applications. Alginate based hydrogels were designed as an oral drug carrier and investigated for the drug release study in biomedical fields especially the colon-targeted system. Structural changes of synthesized hydrogel have been characterized using Fourier transform-infrared spectroscopy (FT-IR), scanning electron microscopy (SEM) and thermogravimetric analysis (TGA) devices. Hydrogels have been studied for their water absorption behavior under the influence of various monomer compositions and changing ambient conditions such as salt, pH and temperature. In this study, diclofenac sodium was used as a model drug to investigate the in vitro release behavior at simulated intestinal (pH 7.0) and gastric fluid (pH 1.2). Lastly, the antibacterial effect of hydrogels and drug-loaded hydrogels was characterized using a disc diffusion method against Gram-positive and Gram-negative bacteria. The suitability of controlled drug release for the use of these new hydrogels in the pharmaceutical and biomedical field has been investigated and our results have shown that the produced hydrogels are promising materials for developing pH-controlled drug delivery devices like capsules for oral use.

Keywords Alginate · Hydrogel · Drug release · Swelling · Antimicrobial

Introduction

Hydrogels are crosslinked network structures that have the ability to hold water by swelling in aqueous media due to the presence of hydrophilic groups like carboxyl groups, sulfonic acid groups and hydroxyl groups while preserving their three-dimensional structure. Their flexible and soft structures can mimic extracellular matrices which explains the large biomedical interest in hydrogels. In addition to chemical crosslinking of hydrogels, physical crosslinks may form with noncovalent interactions (like hydrophobic or ionic interactions, hydrogen bonds) between polymeric chains [1–5]. Additionally, hydrogels can contain groups in their structure with sensor properties. Due to these groups in the structure, they respond to a variety of changes occurring in the environmental conditions like pH, temperature, ionic power, light, electrical and magnetic fields with adjustable physicochemical properties like swelling/shrinking, degradation and permeability in short periods of time. These types of polymers are called 'smart polymers' or 'stimuli-responsive polymers' [6–8].

If one of the polymers with different properties contains crosslinks, while the other does not, these are called semi-interpenetrating polymer networks (semi-IPN). Here, with the aim of changing the features of polysaccharide-based hydrogels playing a primary role due to biocompatibility and overcoming the disadvantages of single polymer networks, it is possible to obtain multicomponent polymer materials with a variety of developed features. Thus, hydrogels gain properties increasing gel strength like better thermal stability, mechanical features and chemical resistance, in addition to including structures that can increase the water absorption and salt resistance of the hydrogel, ensuring the materials obtained meet all requirements for performance in humans [9–11]. In recent times studies have been widely performed about the use of semi-IPN polysaccharide hydrogels in many important biomedical and pharmaceutical fields especially as drug/protein

✉ Pinar Ilgin
pinarilgin@comu.edu.tr; pinarilgin2014@gmail.com

[1] Department of Chemistry and Chemical Processing Technologies, Lapseki Vocational School, Canakkale Onsekiz Mart University, Canakkale/Lapseki, Turkey

[2] Laboratory of Inorganic Materials, Department of Chemistry, Faculty of Science and Arts, Canakkale Onsekiz Mart University, Canakkale, Turkey

[3] Department of Bioengineering, Faculty of Engineering, Canakkale Onsekiz Mart University, Canakkale, Turkey

delivery systems, in addition to as scaffolds for skin, cartilage, bone and cartilage tissues in tissue engineering [12–19].

Controlled drug delivery systems were developed to overcome the limitations of regular medication formulations. The perfect features of semi-IPN hydrogels for controlled and targeted drug administration applications have led them to be the perfect choice due to providing important advantages. Due to porous structures, hydrogels are very permeable for different drug types and as a result can be easily loaded with these drugs. In appropriate conditions, drug release occurs with the desired kinetics in a certain active region with physical stimuli like pH and temperature [20–25].

Among polysaccharides, alginate is obtained as polymer in nature in brown marine algae and some bacteria. It has flat chain molecular structure and the structure contains an anionic natural macromolecule comprising (1 → 4) linked β-D mannuronic acid and α-L-guluronic acid units. Due to advantages like the relatively low cost of creation, and its nontoxic, biologically compatible and biologically degradable nature, Na-alg is one of the polysaccharides most commonly chosen for hydrogel design. As a result, many studies have been performed with Na-alg-based hydrogels especially in pharmacology as drug delivery devices [26–29]. Dadfar et al. prepared semi-IPN of sodium alginate, N-isopropylacrylamide and N-ethylmaleamic acid and used this hydrogel for controlled release of doxorubicin hydrochloride as a model anticancer drug in a drug delivery system [30]. Zhang et al. synthesized one IPN with polyvinyl alcohol and sodium alginate, adopting two physical crosslinking methods of Ca^{2+} crosslinking and freezing thawing, and used composite hydrogels for controlled release of bovine serum albumin and salicylic acid [31]. Khalid et al. obtained crosslinked sodium alginate-graft-poly(acrylic acid) pH sensitive hydrogels for controlled delivery of loxoprofen sodium hydrate in release studies. Maximum swelling, drug loading and release profiles for these hydrogels were observed at pH 7.4 [32].

PVA is a water-soluble synthetic polymer which includes high chemical and mechanical strength, transparency, good biocompatibility, biodegradability and good film-forming ability among its unrivalled features [33]. The cationic monomer of 3-[(methacryloylamino) propyl trimethylammonium chloride] (MAPTAC) and anionic monomer of methacrylic acid (MA) are commonly chosen for preparation of polymers responsive to pH stimuli [34, 35]. Again, hydrogels based on 2-hydroxyethyl methacrylate (HEMA) copolymers are commonly used in biomedical applications [36].

The main theme of this study is to develop and characterize semi-interpenetrating polymer network hydrogels by adjusting the physical and biological properties of the biodegradable and biocompatible alginate with surface functionalization with the aid of monomers containing a variety of functional groups like HEMA, MAPTAC and MA. Na-alg and derivatives are among promising candidates for the preparation of networks ensuring continuous drug release. These new systems were researched for suitability to controlled drug release for use in pharmaceutical and biomedical fields.

Materials and methods

Materials

Important materials used during synthesis of the hydrogel of this study are as follows: [3-(methacryloylamino)propyl] trimethylammonium chloride (here MAPTAC) (50 wt.% in H_2O) as a major monomer, methacrylic acid (here MA) (99%) as a major monomer, 2-hydroxyethyl methacrylate (HEMA) (97%) as a minor monomer, N,N′-methylenebisacrylamide (here, MBA) (99%) as a crosslinker, ammonium persulfate (APS) (98%) as a initiator, and N,N,N′,N′-tetramethylethylenediamine (TEMED) (99%) as an accelerator obtained from Sigma-Aldrich (Steinheim, Germany). Polyvinyl alcohol (PVA) with molecular weight 31,000 g/mol as a stabilizer was obtained from Carl Roth. Alginic acid sodium salt (Na-alg) from brown algae was a white to light beige powder and was obtained from Carl Roth (Karlsruhe, Germany). Amoxicillin (here AMX, >90%), trimethoprim (here TMP, 99%), scolapamine hydrobromide trihydrate (here Sco, 99%), and diclofenac sodium (here Dc, 98%) as model drugs were purchased from Sigma-Aldrich and Acros Organics. Tryptic soy broth (TSB) and tryptic soy agar (TSA) were purchased from Merck. All other materials were of analytical grade and were used without additional purification. Distilled water was used all experimental studies.

Synthesis of semi-IPN hydrogels

The natural polymer of 2.0% (*w*/*w*) aqueous Na-alg solution was mixed for 1 day with a magnetic stirrer at 25 °C. With the aim of chemical stability, 5.0% (w/w) aqueous polyvinyl alcohol (PVA) solution was stirred for 2 h with a magnetic stirrer at 95 °C.

For the synthesis of H1 hydrogel, in brief; 0.024 g (0.8% $w_{MBA}/w_{monomer}$) MBA as a crosslinker were added to the prepared polymer solution containing 1.0 g HEMA monomer, 1.0 g MAPTAC monomer, 1.0 g MA monomer, 5.0 g Na-alg solution, 1.0 g PVA solution and 2.0 g distilled water, and the resulting polymer mixture was stored between 30 and 40 °C. Nitrogen gas was used to remove any dissolved oxygen by cleaning the polymer mixture for about 10 min. Finally, to initiate polymerization, 0.5 mL (0.8% $w_{APS}/w_{monomer}$) initiator and 100 μl TEMED added to the continuously mixed mixture. The prepared solution was placed in cylindrical plastic straws with diameter 0.8 cm and left in a water bath for 4 h

at 60 °C for crosslinking. Later, the polymer samples with crosslinking completed were cut to cylinders with 5.0 mm length and washed with water for two days to remove water soluble oligomers, uncrosslinked polymer and unreacted monomers in the hydrogel. After completing the washing procedure, hydrogels were dried in air. The polymeric samples were stored for later use. Table 1 summarizes the composition of the other synthesized hydrogels.

Swelling capacity studies

The swelling behavior of the stimulus sensitive hydrogel is very important as it can predict the release pattern of the hydrogel discs. Hydrogel pieces in the shape of a cylinder with a mass of about 45 mg, with lenght of 4 mm and diameter of 5 mm, were used for swelling studies. The swelling capacity of the obtained semi-IPN hydrogels in different media was investigated with gravimetric analysis and swelling capacity (S) was calculated as g_{water}/g_{gel} using Eq. (1). When measuring swelling capacity, excess water was removed from the hydrogel surface with filter paper and then measured at certain time intervals.

M_d and M_t represent the dry mass of the hydrogel before swelling and the mass of the hydrogel measured at certain times after swelling, respectively.

$$S = (M_t - M_d)/M_d \quad (1)$$

pH 1.2 solution (SGF): 0.034 M NaCl, 3.3 ml of HCl (37%) in 500 mL of deionized water.

Phosphate buffer saline (PBS) solution (SIF, pH 7.0): 0.034 M NaCl, 2.5 g of KH_2PO_4. H_2O, 4.29 g of $Na_2HPO_4.2H_2O$ in 500 ml deionized water.

Yield, gel fraction and sol-gel fraction of the hydrogel

Yield of hydrogel, amount of crosslinked polymer known as gel fraction and amount of uncrosslinked polymer known as sol-gel fraction were investigated with gravimetric analysis and calculated using Eq. (2).

$$\text{Yield}\% = M_c/M_i x100 \quad (2a)$$

$$\text{Gel fraction}\% = M_d/M_c x100 \quad (2b)$$

$$\text{Sol-gel fraction}\% = 100 - \text{gel fraction}\% \quad (2c)$$

M_i, M_c and M_d are the total mass of all the compounds added during hydrogel synthesis, the mass of dried hydrogel without any pretreatment after synthesis, and mass of the dried hydrogel after removal of components not involved in the synthesis by washing, respectively [37].

Drug loading and drug release behavior studies

Dry semi-IPN hydrogels with 45 mg weight were submerged in 45 ml 100 ppm aqueous diclofenac sodium (Dc) solution to load the hydrogels with the drug. The concentration of drug loaded was determined using a UV-Vis spectrophotometer (T80+ UV/VIS Spectrometer, PG Ins. Ltd.). The following equation was used to analyze the efficiency of drug loading [38]:

$$\text{drug load}\ (\%) = \frac{\text{Total drug} - \text{free drug}}{\text{Total drug}} x100 \quad (3a)$$

Drug release from semi-IPN hydrogels was investigated at physiologic temperature (37 °C) in media with different pHs (pH 1.2 and pH 7.0). After drug loading into dry semi-IPN hydrogels of 45 mg weight, they were left in 5 mL buffer solutions. Once every hour the buffer solution was exchanged with fresh solution and the drug concentration released from hydrogels was measured using a UV spectrophotometer at 276 nm. The percentage drug release was calculated using the following equation [38]:

$$\text{drug release}\ (\%) = \frac{\text{Released drug from hydrogel}}{\text{Total drug in the hydrogel}} x100 \quad (3b)$$

Antimicrobial activity studies

The antibacterial effect of semi-IPN hydrogels both loaded with drugs and without was tested against the gram negative bacterial strain of *Escherichia coli* (*E. coli*, ATCC 8739) and gram positive bacterial strains of *Bacillus subtilus* (*B. subtilus*, DSM 347) and *Staphylococcus aureus* (*S. aureus*, ATCC

Table 1 The synthesis compositions of hydrogels of Na-alg/PVA/p(MAPTAC-co-HEMA-co-MA)

Hydrogel Code	Na-alg (%2 *w/w*) (g)	PVA (%5 w/w) (g)	MAPTAC (g)	MA (g)	HEMA (g)	MBA (g)	H_2O (mL)	Temed μL
H1	5	1	1	1	1	0.024	2	100
H2	5	1	2	1	1	0.032	2	100
H3	5	1	1	2	1	0.032	3	100

6538) with the agar-disk diffusion experiment. In this method, bacteria are seeded on 15 mL TSB agar and incubated overnight at 37 °C. The bacterial culture (100 μL) is poured on the center of TSA plates and evenly spread with the aid of sterile beads. Before hydrogel disks cut into equal sizes are placed on the agar plates, the hydrogels were sterilized for 15 min with a UV lamp. Later the petri dishes were incubated overnight at 37 °C. The next day, the radius (= (total diameter-hydrogel diameter)/2) of the inhibition zone around samples after incubation was measured with a ruler in cm.

Instrumental characterization

In order to obtain information about the surface features of samples, they were analyzed with a 15 kV JEOL 7100-EDX scanning electron microscope (SEM). For SEM analysis, swollen hydrogels were cut into a thin film and then films were freeze-dried. Finally, then samples were coated with gold/palladium (80/20).

Structural characterization of the prepared hydrogels was completed with Fourier transform-infrared spectroscopy (FT-IR). Measurements were made with a Perkin Elmer 100 spectrometer with ATR device with 16 scans, 4 cm^{-1} resolution and 4000 to 650 cm^{-1} screening intervals.

The thermal characteristics of the hydrogels were determined with a Perkin Elmer TGA 8000 device. For this, TG curves were measured in N_2 environment, 30–1000 °C temperature intervals at 10 °C/min heating rate.

Results and discussion

Synthesis and characterization studies

In the synthesis process of the novel semi-IPN hydrogel, free-radical copolymerization of MA, HEMA and MAPTAC monomers in the presence of Na-alg using MBA as a cross-linker under a nitrogen atmosphere and penetration of PVA chains into the hydrogel network occurred simultaneously in an aqueous solution. The plausible reaction mechanism is shown in Fig. 1. The penetration of PVA chains into the polymeric matrix can significantly increase the chemical resistance and mechanical strength of the network due to the additional hydrogen bonding interactions [33]. A digital photograph of the synthesized hydrogels (Na-alg/PVA/p(MAPTAC-co-

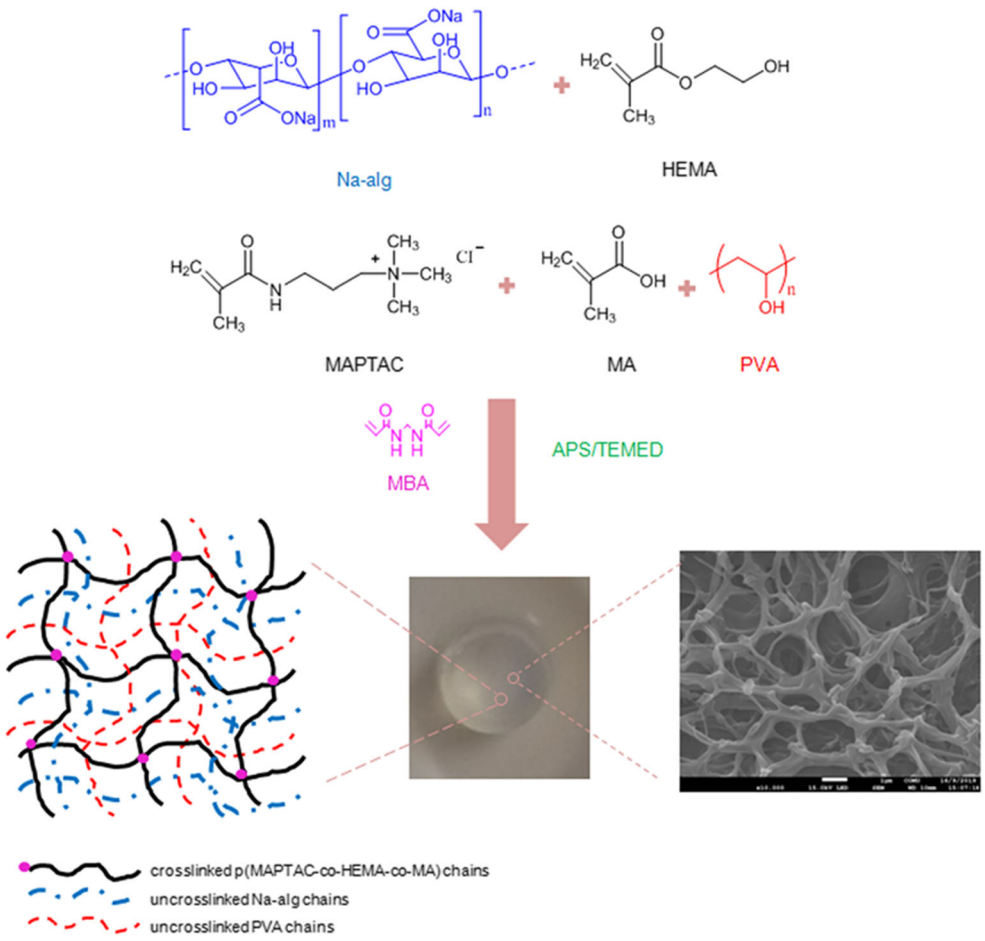

Fig. 1 Schematic representation of the formation of semi-IPN hydrogels and chemical structures of components forming hydrogels

HEMA-co-MA)) in their dry and water-swollen form is given in Fig. 2. Here, H1 is soft and opaque, H2 is soft, brittle and transparent, and H3 is hard and opaque. The structure of the semi-IPN hydrogel was characterized by SEM, FT-IR and TGA devices, and swelling studies. The effect of various parameters such as temperature, time and pH of the medium on swelling ability was studied.

The gel fraction %, sol-gel fraction % and yield % were also calculated and the results are presented in Fig. 3 for obtained hydrogels. Determining the amount of crosslinked and uncrosslinked polymer in the hydrogel is one of its precursors for hydrogel synthesis. For this, gel and sol-gel fraction analyses were done. It was found that hydrogels were obtained with high yield and gel fraction. The results were calculated as about 84, 80 and 76% in the gel fraction of hydrogels at the highest H3, the second-highest H1 and at least H2, respectively. Figure shows that as the amount of MA in the composition of the hydrogel increases the gel fraction also increases. This may be due to the intermolecular H-bond. For the synthesis process, it can be said that the reactants in the feed polymer mixture provide effective active sites for the free radical polymerization reaction and the crosslinking reaction is highly effective.

The internal morphology of freeze-dried swollen semi-IPN hydrogels is shown in SEM photographs in Fig. 4(a-c). As seen in the figure, all semi-IPN displays linked porous structures. The mean pore size in semi-IPN hydrogels appeared to be larger in H2 and H1, and smaller in H3. This tendency may be related to the swelling capacities of semi-IPN hydrogels discussed below. The increase in MA ratio in the H3 hydrogel increased the carboxylic acid groups acting as the source of H-bonds in the network structure. Thus, the hydrophilicity of the hydrogel network reduced and this caused a reduction in water content and limited the migration of water into the network structure. This result also shows the pore sizes in the obtained semi-IPN hydrogels can be adjusted by changing the monomer composition ratios. Hydrogels with adjustable pore structures allow drug-holding efficacy and settable drug release rates. Additionally, large pores ease solvent intake and make spread of the content easier.

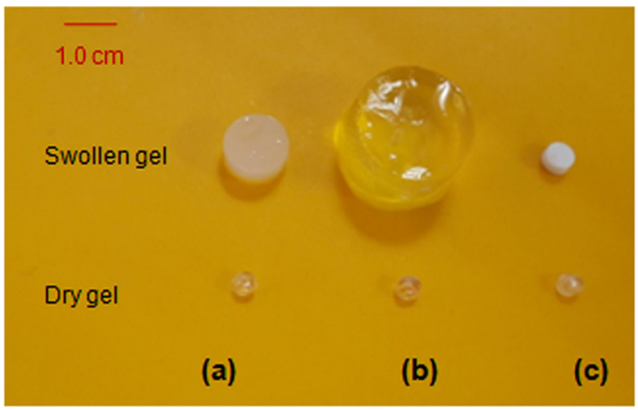

Fig. 2 Digital photograph of dry and swollen semi-IPN hydrogels (**a**) H1 (**b**) H2 (**c**) H3

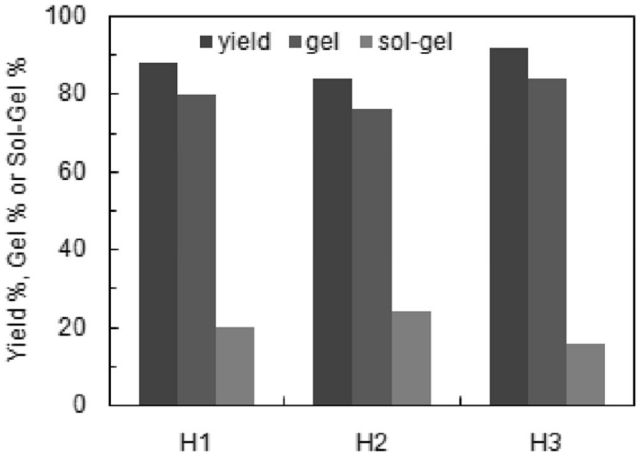

Fig. 3 Effect of hydrogel compositions (H1, H2, H3) on the yield % or gel fraction % and sol- gel fraction %

Figure 5 shows the FT-IR spectra for semi-IPN hydrogel, Na-alg and other components forming the network structure. The band positions of a variety of functional groups in Na-alg, PVA, MAPTAC, HEMA and MA display displacements occurring linked to electrostatic interactions in the FT-IR spectrum of the semi-IPN hydrogel. The peaks at 1482 cm^{-1} and 965 cm^{-1} are attributed C-H symmetric bending of the methyl groups of quaternary ammonium in MAPTAC and the C-N stretching vibration of MAPTAC [34]. The peak around 1707 cm^{-1} was assigned to the C=O stretching vibration of HEMA, MAPTAC and MA. A characteristic peak of Na-alg was represented at 1169 cm^{-1} which indicates glycosidic linkage in its polysaccharide structure [39]. Polymerization was also proven by the presence of strong bands at 2930 cm^{-1} corresponding to the -OH stretching of PVA. Due to the obtained results, the prepared alginate-based semi-interpenetrating polymeric network structure hydrogel was shown to have been successfully obtained.

The TGA curves for Na-alg and semi-IPN hydrogels are given in Fig. 6. The TGA curves for Na-alg and semi-IPN hydrogels display three main degradation stages. The water content of Na-alg and semi-IPN hydrogels (16.3% and 9.7%, respectively) was identified in the weight loss between 30 and 172 °C. Here, humidity is considered to be the total of water remaining in the sample structures in spite of drying before the procedure and water taken from the environment due to the hydrophilic property of the structures. From the TGA thermograms in the interval from 172 to 620 °C, the formation of main products of degradation of Na-alg was due to depolymerization of Na-alg. For semi-IPN hydrogels, 22% weight loss occurred in the interval 175–364 °C while 68% weight loss occurred from 365 to 500 °C. These are considered to be due to depolymerization of Na-alg and degradation of copolymers in the structure, respectively. It was observed that no notable weight loss occurred after 500 °C. When the

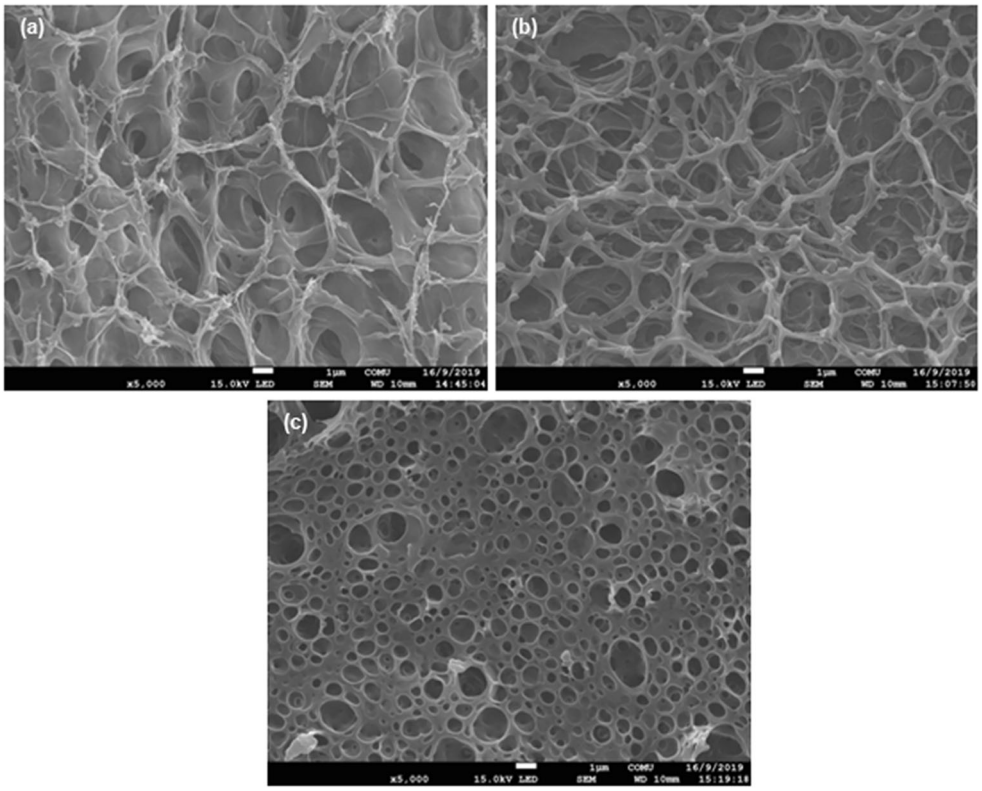

Fig. 4 SEM photograph of freeze-dried swollen semi-IPN hydrogels (**a**) H1 (**b**) H2 (**c**) H3

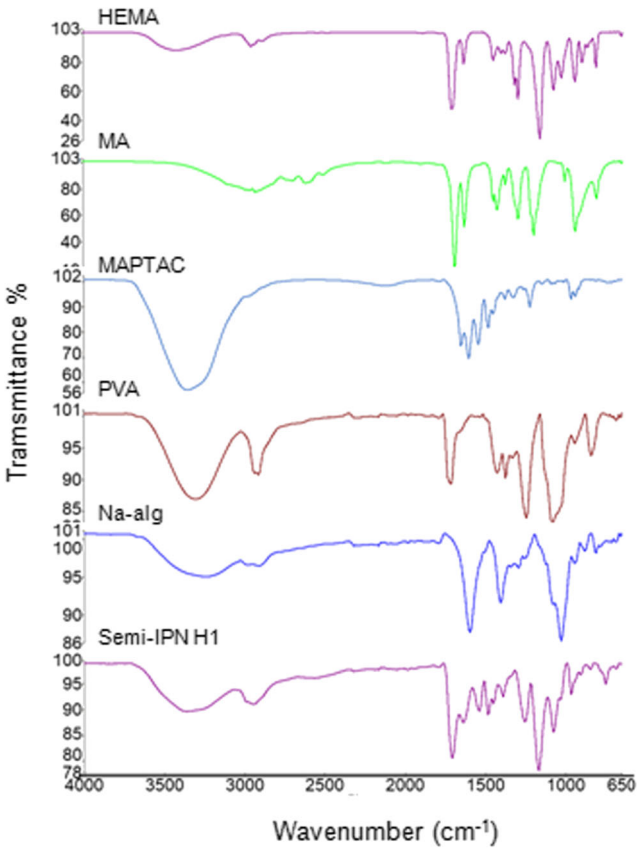

Fig. 5 FT-IR spectra of semi-IPN hydrogel and hydrogel-forming components

temperature reached 800 °C, the hydrogel had lost 99.7% of its initial weight. For natural Na-alg, the curve from 620 to 800 °C may be linked to mild mass loss and partial degradation of interval sodium carbonate which led to formation of carbon dioxide and sodium oxide [40]. The TGA results show the formation of semi-IPN between Na-alg and other compounds. The thermal stability of semi-IPN samples was observed to increase.

Figure 7 shows the effect of different crosslinker ratio on swelling capacity of semi-IPN containing MBA crosslinker. The results show that increasing crosslinker density caused reduced swelling capacity of H1 hydrogel. The reason for this is

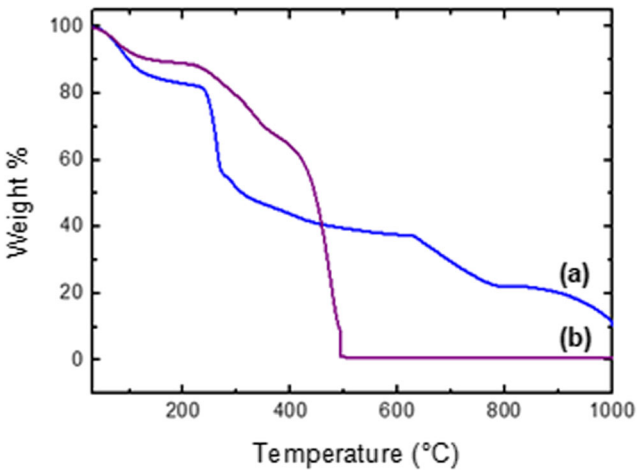

Fig. 6 TGA curves of (**a**) Na-alg and (**b**) semi-IPN hydrogel (H1)

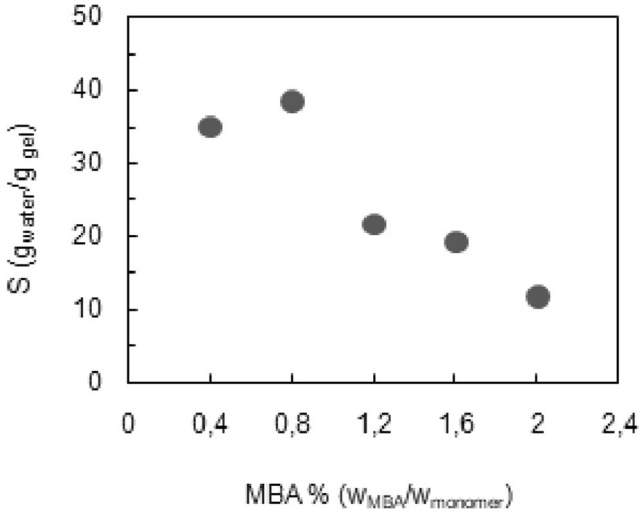

Fig. 7 Swelling capacity of the semi-IPN hydrogel (H1) against the varying crosslinker ratio

that as the amount of crosslinker increases, the interval between polymer chains reduces; thus, the hydrogel structure forms a denser network and absorbs water less [41]. Additionally, for similar crosslinking situations, H1, H2 and H3 hydrogels were prepared with fixed amounts of MBA. For this the MBA amount (according to monomer ratio) was chosen as 0.8%.

According to Fig. 8, all hydrogels were observed to have significant differences in swelling capacities. Semi-IPN hydrogels containing MAPTAC, which is more hydrophilic than MA, are expected to have increased swelling capacity due to increased MAPTAC amounts. As a result, as the number of hydrophilic groups increases, the swelling capacity increases. In Fig. 8, the H2 gel with highest MAPTAC ratio has highest swelling capacity, while H3 gel with higher MA ratio has lowest swelling capacity due to strong hydrogen bond formation between carboxylic acid groups and hydroxyl groups in the network structure. With the increase in MAPTAC concentration, looser hydrogel networks with higher swelling values were obtained.

There is benefit to knowing the swelling behavior in solutions to more clearly understand the drug loading and releasing behavior and to investigate the swelling ability of hydrogels in difficult environments like the stomach and intestines. As a result, the swelling behavior of H1, H2 and H3 semi-IPN hydrogels were investigated in distilled water, simulated gastric fluid (SGF: pH 1.2) and simulated intestinal fluid (SIF: pH 7.0). The addition of NaCl (0.034 M) is to preserve the fixed ionic strength of the buffer solutions. In accordance with controlled drug release, swelling media were studied at 37 °C.

Figure 8 shows the swelling capacity of crosslinked hydrogels in pH 1.2 and pH 7.0 media reduced compared to distilled water with the addition of salt to the solution media. The reason for this is due to the increase in concentration difference between mobile ions in the polymer gel and external medium. The quaternary ammonium groups belonging to the cationic monomer of MAPTAC in the H1 hydrogel network form electrostatic repulsion in pH 1.2 media, and electrostatic repulsion between the anionic Na-alg and ionized

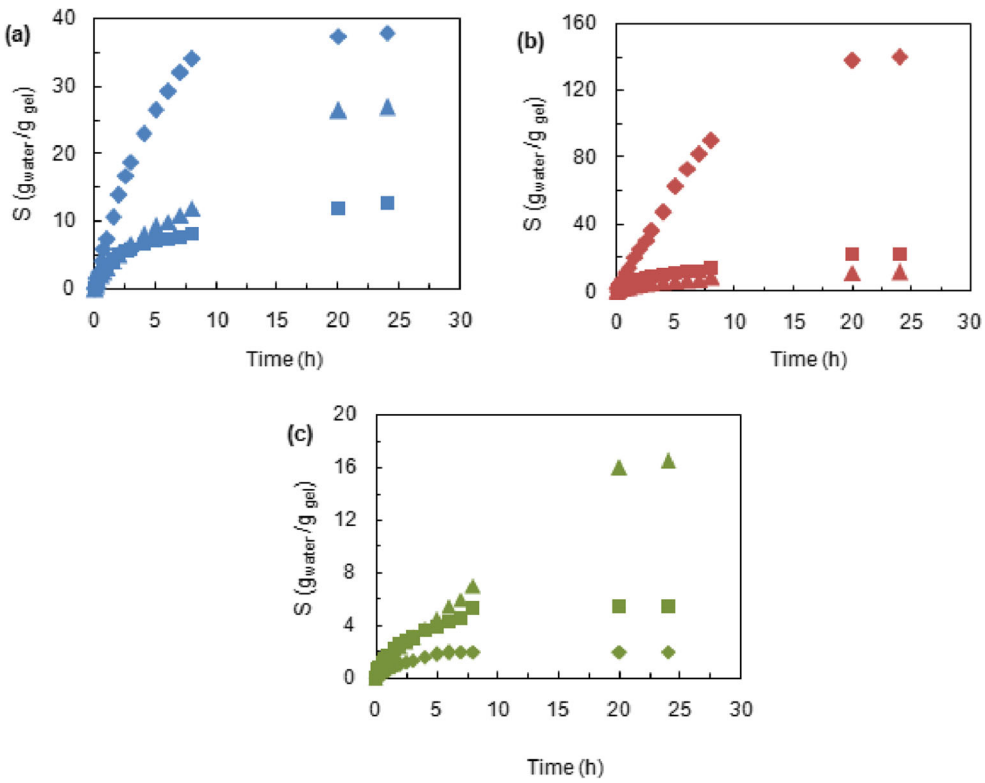

Fig. 8 Swelling capacity of the semi-IPN hydrogel (**a**) H1, (**b**) H2, (**c**) H3 against the time at different media (□ = pH 1.2; Δ = pH 7.0; ◊ = distilled water)

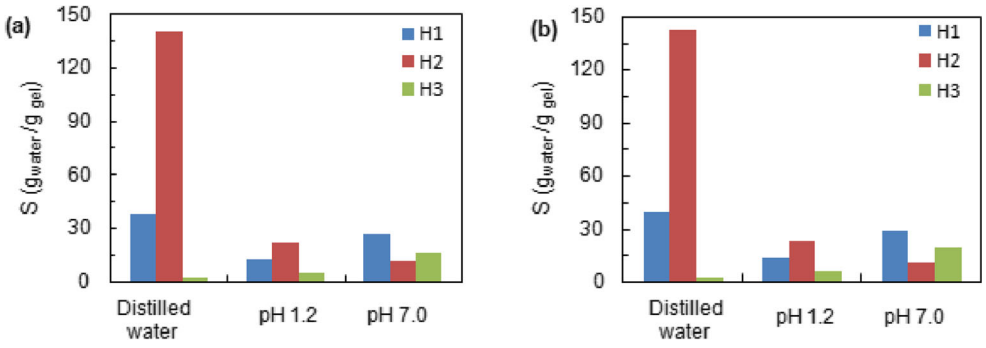

Fig. 9 Semi-IPN hydrogels swelling capacity against distilled water, pH 1.2 and pH 7.0 at (**a**) 25 °C and (**b**) 37 °C

carboxylic groups due to MA occurs in the pH 7.0 medium and thus, the network structures swell (Fig. 8). In pH 1.2 medium with the increase in MAPTAC content in the hydrogel, the H2 gel swells more compared to the pH 7.0 medium (Fig. 8). This is because at pH 1.2 the increase in quaternary ammonium groups in the hydrogel increases electrostatic repulsion between polymer chains and expands the hydrogel structure causing increased swelling. In the pH 7.0 medium, with the increase in MA content in the hydrogel the H3 hydrogel swells more than in the pH 1.2 medium (Fig. 8). In MA carboxylate ions in the carboxylic acid group ionize at pH values higher than the pK_a (4.83) value [42]. Thus, with the increase in carboxylic groups due to Na-alg and MA in the hydrogel, the electrostatic repulsion causing expansion of the network structure increases. This increases the swelling of the gels.

Figure 8 shows that initially water absorption of dry semi-IPN hydrogels increases with time. At the end of 24 h, the equilibrated hydrogels have maximum swelling capacity (g_{water}/g_{gel}) of 38 for H1, 140 for H2, and 1.86 for H3.

The effect of temperature on capacity of swelling is shown in Fig. 9. The swelling capacity at 25 and 37 °C is nearly the same. This may be due to the complicated behavior of compounds contained in semi-IPN hydrogels.

Accordingly based on the best mechanical resistance and swelling capacity evaluations for behavior displayed by hydrogels in swelling media, H1 was chosen for drug loading and drug release studies.

Drug loading and release studies

Diclofenac sodium (Dc) is a nonsteroidal anti-inflammatory drug used for treatment of mild-moderate pain. Here, semi-IPN hydrogels with different functional groups were designed to check the efficacy of drug loading and release of the drug in media. For this strategy, the quaternized ammonium groups from MAPTAC monomer in the semi-IPN hydrogel (H1) network structure form electrostatic interactions between drug and network structure. Together with physical interactions between functional groups in the network structure of semi-IPN hydrogels and drug molecules, hydrogen bond interactions especially contribute to encapsulation [43]. Thus, high affinity interactions are obtained increasing the efficiency of drug loading. Using the swelling-diffusion approach, drugs were loaded into the hydrogel matrix from aqueous solutions at neutral pH. The drug loading capacity for semi-IPN hydrogels was calculated as 22.8%.

Figure 10 shows the cumulative drug release profiles for semi-IPN hydrogel (H1). In vitro release experiments were completed in simulated intestinal fluid (SIF, pH 7.0) and simulated gastric fluid (SGF, pH 1.2) at 37 °C. As described in the figure, there was 4.5% release of diclofenac sodium from semi-IPN hydrogels at pH 1.2 in the first three hours and 95% release at pH 7.0 at the end of twenty hours. In acidic medium the drug release from the hydrogel was limited. This limitation may be linked to low swelling due to lack of ionization of carboxyl groups in the H1 hydrogel network structure in acidic media, and to low solubility of the drug in acidic media (pKa 4.6) [44, 45].

When the medium pH is 7.0, the drug release from semi-IPN hydrogels was clearly observed. The reason for this is that as pH value increases, the swelling due to ionization of carboxyl groups in the network structure benefits release of the loaded drug. In this situation, drug molecules are easily released and spread through the medium and rapid release may occur. At pH 7.0 an initial release effect was observed. This

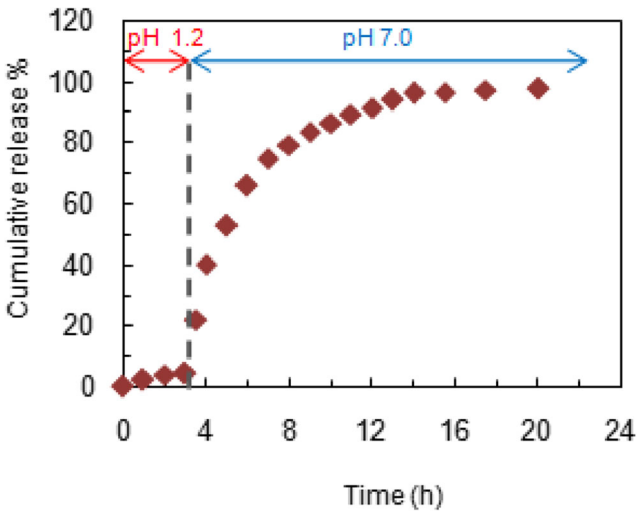

Fig. 10 Time dependent percentage drug release curve for semi-IPN hydrogels (H1) at pH 1.2 and pH 7.0 at 37 °C

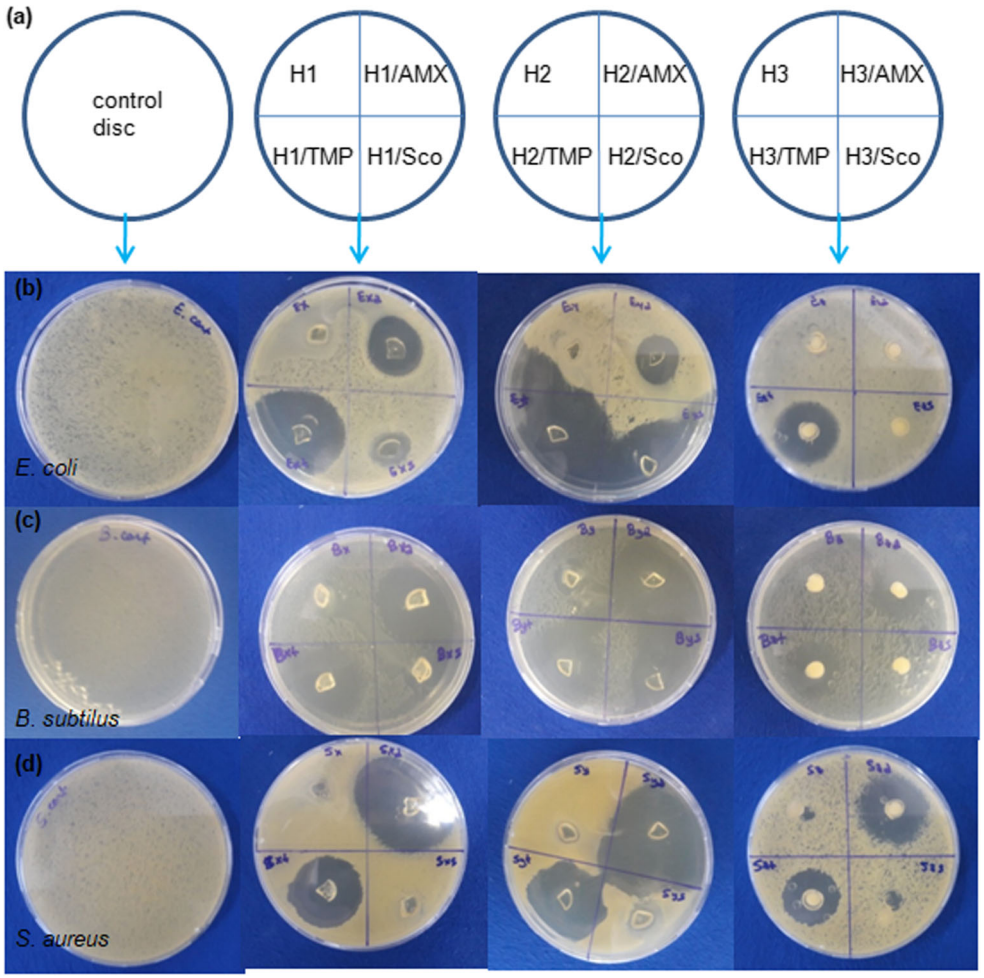

Fig. 11 Digital photographs of antimicrobial activity tests of drug-loaded and unloaded semi-IPN hydrogels (**a**) Schematic representation of the test application for control disc, H1, H2 and H3 hydrogels (top to bottom), for the bacteria applied (**b**) *E. coli*. (**c**) *B. subtilus* (**d**) *S. aureus*

may be linked to the diffusion of the drug resulting from rapid swelling of the surface of the gel matrix and additionally, rapid dissolution of drug directly adsorbed towards the surface of the gel matrix in the medium [45].

Table 2 The inhibition zone radius (cm) of hydrogels and drug-loaded hydrogels

Sample	*E. coli*	*B. subtilus*	*S. aureus*
H1	–	0.5	–
H1/AMX	1.0	1.3	2.4
H1/TMP	1.6	1.3	1.1
H1/Sco	0.5	0.6	–
H2	–	0.5	–
H2/ AMX	0.9	2.5	2.0
H2/TMP	2.3	1.3	1.5
H2/Sco	1.8	0.6	0.6
H3	–	–	–
H3/ AMX	–	1.0	1.1
H3/TMP	1.1	0.9	0.9
H3/Sco	–	–	–

The results show this carrier displays ideal features for release of negligible amounts of Dc in the stomach and release of effective dose amounts in the intestinal environment when administered by the oral route. Semi-IPN hydrogels with 1/1/1 monomer ratio offer a suitable controlled release profile and we identified that Dc release can be controlled by simply adjusting the pH value.

Antibacterial studies of semi-IPN hydrogels

Materials displaying antibacterial properties are important in biomedical research due to effective inhibition of bacterial infections. The antibacterial efficacy of semi-IPN hydrogels containing different MAPTAC/HEMA/MA ratios with controlled release profile and drug-loaded semi-IPN hydrogels were tested against select microorganisms (*E. coli, B. subtilus, S. aureus*) with the disk diffusion method. Antimicrobial activities of all samples reported and the digital photographs are shown in Fig. 11 with zone radii presented in Table 2. For all tested microorganisms, the semi-IPN hydrogel not including any antimicrobial agent used as control had no obvious inhibition zone around the disk. The effect of the hydrogel

remained limited to the area of contact of the disk with the surface and it was found to have its own antimicrobial activity. This may be considered as proof that the obtained semi-IPN hydrogels do not have harmful effects. The antibacterial activity may be linked to the potential cationic MAPTAC groups. Material containing quaternized ammonium was previously reported to have antimicrobial activity [46]. When drugs enter the hydrogel composition, there is a very significant effect on antibacterial activity. Three model drugs were chosen for drug loading with different efficacy; the antimuscarinic scopolamine, and the antibiotics trimethoprim and amoxicillin. Addition of different drugs to the semi-IPN promoted antimicrobial activity against all microorganisms. The inhibition zones around the drug-loaded hydrogels were observed to have high diameters independent of the mixture components for all bacteria. As seen in the figure, it was confirmed that the majority of the three different bacterial types were killed. The data is given in the table. Drugs released from drug-loaded gels entered interactions with the active bacterial nuclei preventing growth and finally causing death. As a result, the strong antimicrobial results for the newly-produced semi-IPN samples show this material can be recommended for potential use in the field of antimicrobial biomaterials.

Conclusion

In this study, pH-responsive semi-interpenetrating polymer network hydrogels by adjusting the physical and biological properties of the biodegradable and biocompatible alginate with surface functionalization with the aid of monomers containing a variety of functional groups like HEMA, MAPTAC and MA were developed and characterized. The addition of PVA and HEMA improved mechanical features and biocompatibility, targeting the provision of new polymers with better physical and chemical properties. As a result of these changes materials with new physicochemical features were obtained. After comparison with different polymeric systems, these new hydrogels formed new material with completely different properties compared to the initial polymer of Na-alg. These newly-obtained materials have thermal and chemical resistance, can be stored in environmental temperatures and additionally have low toxicity. Na-alg and derivatives are among promising candidates for the preparation of networks ensuring continuous drug release. We can suggest that these new hydrogels can be well evaluated as an intelligent drug release platform for pH controlled drug release, especially in oral use.

Acknowledgements This work was financially supported by Çanakkale Onsekiz Mart University the Scientific Research Coordination Unit (Project number: FBA-2018-2575).

References

1. Elsayed MM (2019) Hydrogel preparation technologies: relevance kinetics, thermodynamics and scaling up aspects. J Polym Environ 27(4):871–891. https://doi.org/10.1007/s10924-019-01376-4
2. Zhou M, Ye X, Liu K, Hu J, Qian X (2015) Tunable thermo-responsive supramolecular hydrogel: design, characterization, and drug release. J Polym Res 22(170):1–8. https://doi.org/10.1007/s10965-015-0804-5
3. Wei W, Meng C, Wang Y, Huang Y, Du W, Li H, Liu Y, Song H, Tang F (2019) The interaction between self – assembling peptides and emodin and the controlled release of emodin from in-situ hydrogel. Artif Cell Nanomed Biotech 47(1):3961–3975. https://doi.org/10.1080/21691401.2019.1673768
4. Papavasiliou G, Sokic S, Turturro M (2012) Synthetic PEG hydrogels as extracellular matrix mimics for tissue engineering applications. Biotechnology-molecular studies and novel applications for improved quality of human life. InTech, London, UK, pp 111–134. https://doi.org/10.5772/31695
5. Ma X, Wen G (2020) Development history and synthesis of superabsorbent polymers: a review. J Polym Res 27:136. https://doi.org/10.1007/s10965-020-02097-2
6. El-Sherbiny IM, Khalil IA, Ali IH (2018) Updates on stimuli-responsive polymers: synthesis approaches and features. In: Thakur VK, Thakur MK (eds) Polymer Gels, vol 18. Springer Singapore, Singapore, pp 129–146. https://doi.org/10.1007/978-981-10-6086-1_4
7. Löwenberg C, Balk M, Wischke C, Behl M, Lendlein A (2017) Shape-memory hydrogels: evolution of structural principles to enable shape switching of hydrophilic polymer networks. Acc Chem Res 50(4):723–732. https://doi.org/10.1021/acs.accounts.6b00584
8. Wells CM, Harris M, Choi L, Murali VP, Guerra FD, Jennings JA (2019) Stimuli-responsive drug release from smart polymers. JFB 10(3):34. https://doi.org/10.3390/jfb10030034
9. Nie J, Pei B, Wang Z, Hu Q (2019) Construction of ordered structure in polysaccharide hydrogel: a review. Carbohydr Polym 205: 225–235. https://doi.org/10.1016/j.carbpol.2018.10.033
10. Sami El-banna F, Mahfouz ME, Leporatti S, El-Kemary M, Hanafy NAN (2019) Chitosan as a natural copolymer with unique properties for the development of hydrogels. App Sci 9(11):2193. https://doi.org/10.3390/app9112193
11. Thakur S, Thakur VK, Arotiba OA (2018) History, classification, properties and application of hydrogels: an overview. In: Thakur VK, Thakur MK (eds) Hydrogels, vol 93. Springer Singapore, Singapore, pp 29–50. https://doi.org/10.1007/978-981-10-6077-9_2
12. Shitole AA, Raut PW, Khandwekar A, Sharma N, Baruah M (2019) Design and engineering of polyvinyl alcohol based biomimetic hydrogels for wound healing and repair. J Polym Res 26: 201. https://doi.org/10.1007/s10965-019-1874-6
13. Alvarez-Lorenzo C, Concheiro A (2019) Smart drug release from medical devices. J Pharmacol Exp Ther 370(3):544–554. https://doi.org/10.1124/jpet.119.257220
14. Lin D, Lei L, Shi S, Li X (2019) Stimulus-responsive hydrogel for ophthalmic drug delivery. Macromol Biosci 19(6):1900001. https://doi.org/10.1002/mabi.201900001
15. Altomare L, Bonetti L, Campiglio CE, De Nardo L, Draghi L, Tana F, Farè S (2018) Biopolymer-based strategies in the design of smart medical devices and artificial organs. IJAO 41(6) 337-359.: https://doi.org/10.1177/0391398818765
16. Zhu T, Mao J, Cheng Y, Liu H, Lv L, Ge M, Li S, Huang J, Chen Z, Li H, Yang L, Lai Y (2019) Recent progress of polysaccharide-based hydrogel interfaces for wound healing and tissue engineering. Adv Mater Interfaces 6(17):1900761. https://doi.org/10.1002/admi.201900761

17. Narayanaswamy R, Torchilin VP (2019) Hydrogels and their applications in targeted drug delivery. Molecules 24(3):603. https://doi.org/10.3390/molecules24030603
18. Hussain MA, Kiran L, Haseeb MT, Hussain I, Hussain SZ (2020) Citric acid crosslinking of mucilage from Cydonia oblonga engenders a superabsorbent, pH-sensitive and biocompatible polysaccharide offering on-off swelling and zero-order drug release. J Polym Res 27:49. https://doi.org/10.1007/s10965-020-2025-9
19. Palem RR, Shimoga G, Rao KK, Lee S-H, Kang TJ (2020) Guar gum graft polymer-based silver nanocomposite hydrogels: synthesis, characterization and its biomedical applications. J Polym Res 27:68. https://doi.org/10.1007/s10965-020-2026-8
20. Ozay O, Ilgin P, Ozay H, Gungor Z, Yilmaz B, Kıvanç MR (2020) The preparation of various shapes and porosities of hydroxyethyl starch/p(HEMA-co-NVP) IPN hydrogels as programmable carrier for drug delivery. J Macromol Sci Part A Pure Appl Chem 57(5): 379–387. https://doi.org/10.1080/10601325.2019.1700803
21. Ijaz H, Tulain UR (2019) Development of interpenetrating polymeric network for controlled drug delivery and its evaluation. Intern J Polym Mat Polym Biomat 68(18):1099–1107. https://doi.org/10.1080/00914037.2018.1534110
22. Mignon A, de Belie N, Dubruel P, Vlierberghe SV (2019) Superabsorbent polymers: a review on the characteristics and applications of synthetic, polysaccharide-based, semi-synthetic and 'smart' derivatives. Eur Polym J 117:165–178. https://doi.org/10.1016/j.eurpolymj.2019.04.054
23. Ilgin P, Ozay H, Ozay O (2019) A new dual stimuli responsive hydrogel: modeling approaches for the prediction of drug loading and release profile. Eur Polym J 113:244–253. https://doi.org/10.1016/j.eurpolymj.2019.02.003
24. Havanur S, Farheenand V, JagadeeshBabu PE (2019) Synthesis and optimization of poly (N,N-diethylacrylamide) hydrogel and evaluation of its anticancer drug doxorubicin's release behavior. Iran Polym J 28:99–112
25. Jalababu R, Rao KK, Rao BS. Reddy KVNS (2020) Dual responsive GG-g-PNPA/PIPAM based novel hydrogels for the controlled release of anti- cancer agent and their swelling and release kinetics. J Polym Res 27: 83. https://doi.org/10.1007/s10965-020-02061-0
26. Wang B, Wan Y, Zheng Y, Lee X, Liu T, Yu Z, Huang J, Ok YS, Chen J, Gao B (2019) Alginate-based composites for environmental applications: a critical review. Crit Rev Environ Sci Technol 49(4):318–356. https://doi.org/10.1080/10643389.2018.1547621
27. Aderibigbe BA, Buyana B (2018) Alginate in wound dressings. Pharmaceutics 10(2):42. https://doi.org/10.3390/pharmaceutics10020042
28. Miles JR, Laughlin TD, Sargus-Patino C, Pannier AK (2017) In vitro porcine blastocyst development in three-dimensional alginate hydrogels. Mol Reprod Dev 84(9):775–787. https://doi.org/10.1002/mrd.22814
29. Giri TK, Thakur D, Alexander A, Ajazuddin BH, Tripathi DK (2012) Alginate based hydrogel as a potential biopolymeric carrier for drug delivery and cell delivery systems: present status and applications. Curr Drug Deliv 9(6):539–555. https://doi.org/10.2174/156720112803529800
30. Dadfar SMR, Pourmahdian S, Tehranchi MM, Dadfar SM (2019) Novel dual-responsive semi-interpenetrating polymer network hydrogels for controlled release of anticancer drugs. J Biomed Mater Res 107(10):2327–2339. https://doi.org/10.1002/jbm.a.36741
31. Zhang S, Han D, Ding Z, Wang X, Zhao D, Hu Y, Xiao X (2019) Fabrication and characterization of one interpenetrating network hydrogel based on sodium alginate and polyvinyl alcohol. J Wuhan Univ Technol Mat Sci Edit 34(3):744–751. https://doi.org/10.1007/s11595-019-2112-0
32. Khalid I, Ahmad M, Usman Minhas M, Barkat K, Sohail M (2018) Cross-linked sodium alginate-g-poly(acrylic acid) structure: a potential hydrogel network for controlled delivery of loxoprofen sodium. Adv Polym Technol 37(4):985–995. https://doi.org/10.1002/adv.21747
33. Bajpai AK, Vishwakarma A, Bajpai J (2019) Synthesis and characterization of amoxicillin loaded poly (vinyl alcohol)-g-poly (acrylamide) (PVA-g-PAM) hydrogels and study of swelling triggered release of antibiotic drug. Polym. Bull. 76(7): 3269-3295. https://doi.org/10.1007/s00289-018-2536-2
34. Kusuktham B (2006) Preparation of interpenetrating polymer network gel beads for dye absorption. J Appl Polym Sci 102(2):1585–1591. https://doi.org/10.1002/app.23882
35. Shabir F, Erum A, Tulain UR, Hussain MA, Ahmad M, Akhter F (2017) Preparation and characterization of pH sensitive crosslinked linseed polysaccharides-co-acrylic acid/methacrylic acid hydrogels for controlled delivery of ketoprofen. Desig Monom Polym 20(1): 485–495. https://doi.org/10.1080/15685551.2017.1368116
36. Sadeghi M (2011) Synthesis of starch-g-poly(acrylic acid-co-2-hydroxy ethyl methacrylate) as a potential pH-sensitive hydrogel-based drug delivery system. Turk J Chem 35:723–733. https://doi.org/10.3906/kim-1103-27
37. Ganguly S, Das NC (2015) Synthesis of a novel pH responsive phyllosilicate loaded polymeric hydrogel based on poly(acrylic acid-co-N-vinylpyrrolidone) and polyethylene glycol for drug delivery: Modelling and kinetics study for the sustained release of an antibiotic drug. RSC Adv 5:18312–18327
38. Pathania D, Verma C, Negi P, Tyagi I, Asif M, Kumar NS, Al-Ghurabi EH, Agarwal S, Gupta VK (2018) Novel nanohydrogel based on itaconic acid grafted tragacanth gum for controlled release of ampicillin. Carbohydr Polym 196:262–271. https://doi.org/10.1016/j.carbpol.2018.05.040
39. Rasool A, Ata S, Islam A, Khan RU (2019) Fabrication of novel carrageenan based stimuli responsive injectable hydrogels for controlled release of cephradine. RSC Adv 9(22):12282–12290. https://doi.org/10.1039/C9RA02130B
40. Cheong M, Zhitomirsky I (2008) Electrodeposition of alginic acid and composite films. Coll Surf A Physicochem Eng Asp 328(1–3): 73–78. https://doi.org/10.1016/j.colsurfa.2008.06.019
41. Pourjavadi A, Farhadpour B, Seidi F (2008) Synthesis and investigation of swelling behavior of grafted alginate/alumina superabsorbent composite. Starch - Stärke 60(9):457–466. https://doi.org/10.1002/star.200800208
42. Şolpan D, Kölge Z (2006) Adsorption of methyl violet in aqueous solutions by poly(N-vinylpyrrolidone-co-methacrylic acid) hydrogels. Radiat Phys Chem 75(1):120–128. https://doi.org/10.1016/j.radphyschem.2005.06.005
43. Abou Taleb MF (2013) Radiation synthesis of multifunctional polymeric hydrogels for oral delivery of insulin. Intern J Biol Macromol 62: 341–347. https://doi.org/10.1016/j.ijbiomac.2013.09.004
44. Yin L, Ding JY, Fei L, He M, Cui F, Tang C, Yin C (2008) Beneficial properties for insulin absorption using superporous hydrogel containing interpenetrating polymer network as oral delivery vehicles. Int J Pharm 350(1–2):220–229. https://doi.org/10.1016/j.ijpharm.2007.08.051
45. Moin A, Hussain T, Gowda DV (2017) Enteric delivery of diclofenac sodium through functionally modified poly(acrylamide-grafted-ghatti gum)-based ph-sensitive hydrogel beads: development, formulation and evaluation. J Young Pharm 9(4):525–536. https://doi.org/10.5530/jyp.2017.9.102
46. Ng VWL, Chan JMW, Sardon H, Ono RJ, García JM, Yang YY, Hedrick JL (2014) Antimicrobial hydrogels: a new weapon in the arsenal against multidrug-resistant infections. Adv Drug Deliv Rev 78:46–62. https://doi.org/10.1016/j.addr.2014.10.028